CO2 storage and conversion to CH4 by wet mechanochemical activation of olivine at room temperature

Contents lists available at ScienceDirect

Powder Technology

journal homepage: http://ees.elsevier.com

CO_2 storage and conversion to CH_4 by wet mechanochemical activation of olivine at room temperature

Nadia Gamba [a,b], Valeria Farina [c], Sebastiano Garroni [c], Gabriele Mulas [c], Fabiana Gennari [a,bd,*]

[a] Consejo Nacional de Investigaciones Científicas y Técnicas (CONICET), R8402AGP, S. C. de Bariloche, Río Negro, Argentina
[b] Centro Atómico Bariloche (CAB-CNEA), R8402AGP, S.C. de Bariloche, Río Negro, Argentina
[c] Dipartimento di Chimica e Farmacia and INSTM, Università degli Studi di Sassari, 07100 Sassari, Italy
[d] Universidad Nacional de Cuyo (UNCuyo), Instituto Balseiro, Av. Bustillo 9500 R8402AGP Bariloche, Río Negro, Argentina

ARTICLE INFO

Article history:
Received 19 June 2020
Received in revised form 24 August 2020
Accepted 21 September 2020
Available online xxx

Keywords
Olivine
Carbon dioxide storage
Carbon dioxide conversion
Magnesium carbonate
Methane
Mechanical milling

ABSTRACT

Wet mechanochemical processing of olivine under a CO_2 atmosphere promotes the CO_2 sequestration in the form of $MgCO_3$ and the CO_2 reduction to CH_4 at room temperature. The effects of milling time and CO_2 pressure on the CO_2 storage and CO_2 reduction were evaluated at lab-scale. Wet mechanochemical introduces progressively significant morphological, structural, microstructural and textural changes in olivine for prolonged milling times, inducing fast carbonation reaction after 15 min of ball milling. Long milling times stimulate the CO_2 conversion to CH_4 and decrease the carbonation reaction rate, because both reactions occurred simultaneously. The CO_2 sequestrated as $MgCO_3$ is about 4.83 wt% and 6.81 wt% for 1.0 atm of CO_2 after 120 min and 180 min of milling using different CO_2 charge strategy. The amount of CO_2 reduced to CH_4 was 24 and 33 mmoles/kg of olivine after 120 min with 1.0 and 1.5 atm of CO_2, respectively. Wet milling of olivine in CO_2 atmosphere is a technique with potential for large-scale carbon mineralization.

1. Introduction

The increase of carbon dioxide concentration in the atmosphere since the industrial revolution up today, has caused detrimental environmental impacts such as the global warming and the ocean acidification [1]. This situation could be mainly attributed to the increasing consumption of fossil fuels around the world. In fact, fossil-fuel power plants are responsible of about one third of the total anthropogenic emissions of carbon dioxide, while other contributors being cement and chemical industries. Therefore, different approaches and technologies for carbon capture, utilization and storage are needed to mitigate the CO_2 emission [2–5].

Carbon Capture and Storage (CCS) and Carbon Capture and Utilization (CCU) technologies are strategies that are attracting the interest of the scientific community [2–5]. Among the proposed carbon capture and storage technologies (CCS), Mineral Carbonation (MC) is one of the safest and permanent methods, which simulates the natural process of mineral weathering. It is based on the reaction of carbon dioxide with silicate minerals containing Mg and/or Ca to form water insoluble carbonates, which are also thermally stable and eco-friendly [6,7]. Suitable materials for this MC process are abundant silicate rocks, such as olivine, one of the most abundant mineral in the Earth's surface. Olivine is an orthosilicate with a general formula $(Fe_xMg_{1-x})_2SiO_4$ representing a complete solid solution between forsterite (Mg_2SiO_4) and fayalite (Fe_2SiO_4), in which the magnesium member is usually dominant (~ 92%). MC of olivine is a thermodynamically favorable process that has been observed in nature [8] and it can be described by the following reaction:

$$Mg_2SiO_4\,(s) + 2CO_2\,(g) \longrightarrow 2MgCO_3\,(s) + SiO_2\,(s) \quad (1)$$

In presence of water, wet carbonation involves the dissolution of CO_2 in aqueous medium and the formation of carbonic acid, which reduces the pH of medium:

$$\begin{aligned} 2CO_2\,(g) + 2H_2O\,(l) &\leftrightarrow 2H_2CO_3\,(aq) \\ &\leftrightarrow 2HCO_3^-\,(aq) + 2H^+\,(aq) \\ &\leftrightarrow 2CO_3^{2-}\,(aq) + 4H^+\,(aq) \end{aligned} \quad (2)$$

The acidic medium favors the dissolution of olivine and Mg^{2+} is released from the mineral:

$$Mg_2SiO_4\,(s) + 4H^+\,(aq) \leftrightarrow 2Mg^{2+}\,(aq) + H_4SiO_4\,(s) \quad (3)$$

* Corresponding author at: Consejo Nacional de Investigaciones Científicas y Técnicas (CONICET), Centro Atómico Bariloche (CNEA) and Universidad Nacional de Cuyo (Instituto Balseiro), Av. Bustillo 9500 R8402AGP Bariloche, Río Negro, Argentina.
E-mail address: gennari@cab.cnea.gov.ar (F. Gennari)

https://doi.org/10.1016/j.powtec.2020.09.039
0032-5910/

Subsequently, the Mg^{+2} ions react with carbonate and the formation of $MgCO_3$ is possible:

$$2Mg^{2+}\ (aq) + 2CO_3{}^{2-}\ (aq) \leftrightarrow 2MgCO_3\ (s) \quad (4)$$

where (g), (l), (aq) and (s) indicate gas, liquid, aqueous and solid state respectively. The natural MC is a very slow process under atmospheric temperature and pressure conditions, which makes this technology not industrially feasible without modifications [9,10]. Therefore, current MC research activities focus on speeding up this process in order to storage CO_2 in an efficient way.

Dissolution of olivine (reaction (3)) is a key step that usually controls the MC reaction rate. Consequently, the factors that modify olivine dissolution like agglomerate size, specific surface area and crystal disorder, impact directly on the kinetics of carbonation process [11–13]. Dissolution of forsterite showed to be dependent on the surface properties like reactive surface sites and the specific surface area. Crystallinity is also a factor that influences the mineral dissolution rates which increases with increasing of Si:O ratio [14,15]. The rate controlling step of dissolution of silicate minerals is the breaking of Si—O bonds and thus amorphization can improve the mineral dissolution kinetics due to disordering of the mineral structure and weakens the Si—O bonds. In this context, one possibility to upgrade olivine dissolution is to modify its structural, microstructural and textural characteristics by mechanical activation [16,17]. Mechanical milling has shown to be an effective tool to improve olivine reactivity by reducing its particle size, grain size and crystallinity, by increasing its surface area and *via* the generation of surface and lattice defects. The excess of energy stored in the solid powders during mechanical activation could reduce the activation energy of carbonation reaction under dry or wet conditions [15,18–20]. In addition, some studies have also noted that milling enhances the reactivity of Mg-silicates by reducing agglomerate size [21,22]. Moreover, it has been demonstrated that milling of olivine under dry and wet conditions introduces different structural and morphological modifications that improve its dissolution [15,17–20]. In fact, by exploring the combination of dry mechanical activation with subsequent wet milling the specific surface of olivine powders was enhanced [23]. It was possible to produce specific surface area of olivine at rates that exceed those obtained by wet milling alone.

MC of olivine in natural environments has been related not only with the formation of carbonates (CCS) but also with CH_4 and hydrocarbons production (CCU) [24–29]. There seems to be a relation between production of H_2 *via* olivine hydrolysis (serpentinization) and the formation of CH_4 and hydrocarbons. In this regard, Neubeck et al. [24] studied the interactions between water and natural olivine in the temperature range of 30 to 70 °C. The experimental evidence suggests that CH_4 and H_2 were formed, and CH_4 formation correlates with olivine dissolution rates. Moreover, Mac Collom et al. have shown that methane and minor amounts of hydrocarbons may be formed in the superficial crust through thermogenic breakdown of biomolecules, Fischer–Tropsch Type (FTT) synthesis from CO or CO_2, and decarboxylation of aqueous acetate [25]. Other studies have noted that methane can be also produced from carbonate [26,27] or from gas-water-rock reactions [28] at high pressures. The results suggest that serpentinization of Mg-rich minerals like forsteritic olivine leads to H_2 production *via* Fe^{2+} oxidation, which forms Fe_3O_4 (magnetite) and serpentine ($Mg_3Si_2O_5(OH)_4$). Experimental studies at 300 °C and above have suggested that abiotic CH_4 synthesis has strong kinetic barriers unless some minerals with Fe and Cr metals act as catalysts [29–31]. Thus, as dissolution of olivine is promoted within a specific range of pressure, temperature and pH conditions, simultaneous CO_2 mineral sequestration and hydrogen/hydrocarbon production could occur.

Our recent work explored the effect of high energetic milling of olivine in CO_2 atmosphere with water addition on both CO_2 storage and CO_2 utilization processes. We demonstrated that mechanochemical milling of olivine in presence of H_2O and CO_2 is efficient to promote the formation of carbonate phases and hydrogen production, with faster kinetics compared with hydrothermal process [32,33]. Mechanochemical treatments of olivine-water in CO_2 atmosphere induces H_2O dissociation and the consequent H_2 formation, which can promote FTT reaction on the olivine surface. CO_2 hydrogenation to obtain mainly CH_4 showed an induction period depending on both CO_2 and H_2 activation. The concentration of CH_4 and other light hydrocarbons was dependent on the experimental setup, the relative amount of olivine/water and the experimental conditions applied [33].

In this work, we assess in the laboratory-scale the potential for the CO_2 storage and CO_2 conversion of natural olivine by mechanochemical activation in CO_2 atmosphere at room temperature. Structural, microstructural and textural changes of olivine during wet mechanochemical reaction were studied and correlated with the CO_2 storage and conversion processes. The effect of CO_2 pressure and milling time on the extension of carbonation reaction and CO_2 reduction was analyzed. The final purpose of this work is to report results useful to understand the potential role of wet mechanochemical processing of olivine as a viable CCU technique.

2. Experimental

2.1. Starting materials and processing

Olivine powders used in this study were provided by Satef (Italy) and originated from Norway. The chemical analysis performed by the supplier indicates the following relative composition, expressed as weight % of oxide: 50.0% MgO, 41.5% SiO_2, 7.3% Fe_2O_3, 0.4% Al_2O_3, 0.3 NiO, 0.29 Cr_2O_3, 0.1 MnO, 0.1% CaO. Carbon Dioxide gas was provided by Linde (5.0).

For wet milling runs, olivine powders (2 g) and deionized water (0.3 mL) were placed in the milling chamber. The mixture was ball milled under different CO_2 pressures using a planetary mill (Fritsch Pulverisette 6). The experimental conditions selected were: ball to power weight ratio of 40:1 and 500 rpm. The milling chamber was provided with a valve to introduce CO_2 gas and connected to a special gas line. The gas line was connected to different gas reservoirs, a vacuum system and two pressure gauges. Consecutive vacuum and charge stages of the CO_2 gas were done to ensure the purity of the reaction gas. Then, a single initial charge of 0.25, 0.5, 1.0 and 1.5 atm of CO_2 pressure was performed for each milling time. For CO_2 pressures lower than 1.0 atm, the total pressure was 1.0 atm using Ar as balance. To perform each wet milling run modifying the milling time and CO_2 pressure, a different olivine sample was used. In particular, four groups of experiments were conducted at 0.25, 0.5, 1.0 and 1.5 atm of CO_2 for 15, 30, 60, 90 and 120 min of milling.

Dry milling runs of 2 g of olivine were performed using two different conditions: 1) 1.0 atm of CO_2 using the same previous protocol of single charge and 2) recharging the CO_2 pressure (1.0 atm) every 30 min of grinding to maximize the CO_2/surface ratio. For dry milling runs, 15 and 120 min (case 1) and total 180 min (for case 2) were carried out. As reference two experiments were carried out: the vial without olivine nor water was ball milled for 30 min in 1.0 atm of CO_2; olivine-water was exposed to 1.0 atm of CO_2 under static conditions.

2.2. Characterization of the solid products and reaction quantification

The starting olivine, the as-milled solid products and the gases produced were analyzed using several experimental techniques. The crystalline structures and the changes in the chemical compositions of the samples after mechanochemical processing were studied by X-ray powder diffraction (XRPD, Bruker D8 Advance) and Fourier-transform infrared spectroscopy (FTIR, Perkin Elmer Spectrum 400) analyses. The

XRPD patterns were obtained in the range of 10° and 80° with CuKα radiation (λ = 1.5406) at 40 kV and 40 mA. The relative fraction of crystalline phase (C_{XRD}) in the as-milled samples was estimated on the basis of the method proposed by Ohlberg and Strickler [34]:

$$C_{XRD} = \frac{U_0}{U_X} \cdot \frac{I_X}{I_0} \quad (5)$$

being U the background level, I the integral intensity of a selected diffraction peak, and the subscripts 0 and *X* represent the as-received sample and the as-milled sample, respectively. The 020 (hkl) peak from the Forsterite was chosen for the calculations as it is one of the few peaks that lends itself to a closer analysis. For the solid state FTIR studies, pressed pellets were prepared by grinding of the samples with dry KBr and the spectra were obtained in the range of 4000–500 cm^{-1} in air.

The nominal carbon content present in the powders after wet milling of olivine in 1.0 atm of CO_2 was determined using Total Carbon Analysis (TCA, LECO CS 230). The amount of CO_2 stored in each run (in grams or in mol) was calculated assuming that the nominal carbon content measured by LECO is due to CO_2 sequestrated by the sample. The wt% of CO_2 stored is the ratio of the weight of CO_2 stored (in grams) to the total weight of the sample (per 100). The mol ratio (in %) of CO_2 stored is defined as the relation between the amount of CO_2 stored (in moles) and the total amount of CO_2 at the beginning of the reaction (in moles). The presence of carbon was also analyzed by Raman spectroscopy with a confocal microscope (LabRAMHR Evolution Raman microscope) at room temperature and using the laser wavelength of 514 nm.

The morphologies of pristine olivine and as-milled olivine were determined by Scanning Electron Microscopy (SEM-FIB, Zeiss, Crossbeam 340). Powders were dispersed onto carbon stick and coated with gold to improve the electrical conductivity. Energy-Dispersive X-ray Spectroscopy (EDXS) was carried out using elemental analyzer to clarify the distribution of C, Mg, O, Si and Fe.

N_2 sorption isotherms were collected on a Micromeritics ASAP 2020 analyzer at −196 °C. Before each measurement, 0.5 g of sample were evacuated at 350 °C overnight. The data were analyzed according to BET and BJH methods to estimate surface area and total pore volume.

The weight changes of wet milled samples in CO_2 atmosphere were measured using thermogravimetric analysis equipment (TGA, PT-1800, Linseis). Samples of about 40 mg were loaded into alumina capsules and heated at 5 °C/min in argon gas flow. Simultaneously, the gases released were analyzed by mass spectroscopy (MS).

2.3. Characterization of the gas products and reaction quantification

The extent of reaction during wet milling of olivine in CO_2 was determined by gas-FTIR analysis using a degassed quartz optical cell with KBr windows. After each milling run, gas samples from the milling chamber were collected and analyzed by gas-FTIR technique. Calibration curves were constructed to determine quantitatively the amount of CH_4 and CO species presented after milling, following the procedure previously reported [35] and using analytical standards mixtures. In addition, gas samples from some specific runs were analyzed by gas chromatography (GC, Agilent Technologies GC System 7820A), using a Thermal Conductivity (TCD) and Flame ionization (FID) detectors. In particular, GC was used to determine the presence of non-active IR species like H_2, in addition to CH_4, CO and CO_2. Quantitative analyses were carried out using calibration curves obtained by injection of analytical standards. Methane and CO yields were quantified using mmol/kg olivine, where the weight of olivine refers to the olivine weight at the beginning of each experiment.

3. Results and discussion

3.1. Structural modifications of olivine after wet milling in CO_2 atmosphere

Structural changes of as-received olivine and the as-milled olivine for different times were studied using XRPD analysis (Fig. 1). A deep structural study of the as-received olivine powders was performed in our previous work [32]. This olivine consists of three phases: the main phase is Forsterite (91 wt%, $Fe_{0.2}Mg_{1.8}SiO_4$), followed by Enstatite ferroan (7.5 wt%, $Fe_{0.2}Mg_{0.8}SiO_3$) and minor amounts of Clinochlore ($Al_{1.84}Fe_{0.5}H_8Mg_{4.5}O_{18}Si_{3.16}$). After 15 min of wet milling under 0.5 atm of CO_2 pressure (Fig. 1), the characteristic peaks of Clinochlore phase disappear, while those corresponding with Forsterite and Enstatite are progressively wider. No other clear change in the nature of the phases was observed from the XRPD patterns due to milling time increase. Wet mechanochemical processing of olivine under CO_2 atmosphere produces refinement of the microstructure of Forsterite as a consequence of milling time progress. In order to analyze quantitatively the structural changes, the characteristic parameters of (020) diffraction peak of Forsterite were shown in Table 1. In general, a 2θ shift to higher angles was observed over milled samples in comparison with the as-received olivine, which indicates a regular and continuous compression of the Forsterite lattice volume. The position of the (020) diffraction peak has a direct correlation with the lattice parameter *b* of the Forsterite phase. These data could indicate a decreasing of the Fe con-

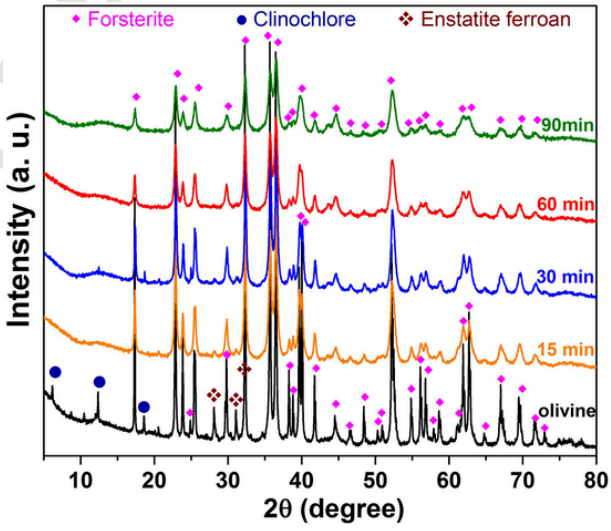

Fig. 1. X-ray powder diffraction patterns of the as-received olivine and the products obtained after wet milling olivine in 0.5 atm of CO_2 for different milling times.

Table 1
Changes in the XRPD parameters of (020) Forsterite peak under different milling conditions (CO_2 pressure, presence/absence of water, time).

CO_2 pressure (atm)	Water/dry	Time(h)	2θ (degree)	I/I_0	FWHM	C_{XRD}
–	–	0	17.339	3.35	0.070	100
0.5	Water	15	17.375	0.89	0.097	25
		30	17.417	0.73	0.098	20
		60	17.366	0.35	0.177	17
		90	17.384	0.21	0.197	12
1	Water	60	17.393	0.36	0.098	10
		90	17.365	0.21	0.157	9
1	Dry	15	17.419	0.78	0.079	17
		120	17.363	0.19	0.197	11

tent in the forsterite–fayalite solid solution of olivine [36,37]. In addition, a continuous broadening of the diffraction peaks and decreasing in the intensity were observed with milling time extension. These changes were quantified through the increase of the full width at half of the maximum height (FWHM) and the reduction of the I/I_0 ratio (I = intensity of the selected peak and I_0 = intensity of background) with extension of milling time. Similar behavior was observed under dry milling conditions. All these parameters indicate that the Forsterite phase suffers structural modifications and becomes partially amorphous due to mechanical activation. As a confirmation, the fraction of crystalline phase C_{XRD} calculated by eq. (5) (Table 1 and Fig.S1) shows a sharp reduction with milling time increase. In fact, Forsterite reduces its crystalline fraction from 100% to about 25% (12%) after 15 min (90 min) of wet milling (Table 1). The amorphisation of olivine due to wet milling is in the order of that measured in previous works (Table 1 and Fig. S1) [16,21,23,38], although there are some differences associated to the milling energy. Moreover, even after prolonged milling, the presence of the main Forsterite diffraction peaks indicates the high resistance to mechanical deformation of olivine.

In order to obtain additional structural information of the olivine after wet milling in CO_2, solid-state FTIR spectra were collected after different milling times under 0.5 atm of CO_2 (Fig. 2). The spectrum of as-received olivine is included for comparison. In all samples, the characteristic bands of Forsterite in the range of 980–1100 cm^{-1}, 860–890 cm^{-1} and 600–615 cm^{-1} associated to SiO_4 stretching and SiO_4 bending modes respectively, were observed [39]. In contrast, two groups of bands were detected in the samples after wet milling. On one hand, the presence of broad peaks at 3440 cm^{-1} and 1635 cm^{-1} ascribed to OH-stretching and -bending modes, respectively, was observed. These bands can be associated with OH groups and water, respectively, absorbed on the olivine surface due to partial serpentinization process occurring by milling. The bonding of water on the olivine surface increases the possibility of olivine dissolution (reactions 3 and 4) [18,19]. On the other hand, $MgCO_3$ formation was confirmed by the identification of double peaks in the region 1350–1600 cm^{-1} (C═O bonds). When the milling time increases, the intensity of $MgCO_3$ peaks seems to increase. However, crystalline $MgCO_3$ was not detected in any XRPD patterns (Fig. 1) probably due to its amorphization during milling. Identification of Si—O bands related to silica formation is ambiguous, because its bands are located in the range 980–1100 cm^{-1}. Similar results were obtained at different CO_2 pressure (see Fig. S2).

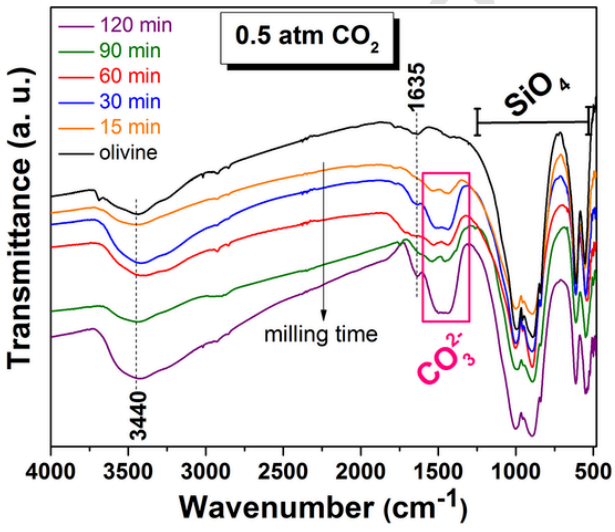

Fig. 2. Solid-phase FTIR spectra of phases after mechanochemical activation of olivine with water under 0.5 atm of CO_2 after different milling times.

3.2. Microstructural/textural studies of olivine after wet milling in CO_2 atmosphere

The as-received olivine suffers strong textural modifications during mechanochemical activation in CO_2 atmosphere (Fig. 3 and Table 2). N_2 absorption/desorption isotherm of the starting olivine shows a typical type II physisorption isotherm, corresponding to non-porous or macroporous material according to IUPAC classification [40]. In contrast, the olivine milled in CO_2 atmosphere both under dry or wet conditions displays an isotherm Type IV, with H3 hysteresis loop in the P/P_0 range 0.5–0.9 (Fig. 3). The specific surface area of olivine increases from 0.5 m^2/g to 33 m^2/g after 60 min of milling under wet condition (Table 2). Further wet milling for 120 min reduces the specific surface area and the cumulative volume of pores (Table 2). This behavior was previously observed for dry milling and usually it is associated with agglomeration of particles after long milling times following the initial particle size reduction [15]. A similar situation could be present in our samples after prolonged milling due to partial dehydration of the powders in CO_2 atmosphere. By applying the BJH method to the desorption branch of the isotherm, the as-milled olivine samples show an average pore size distribution between 3.5 and 3.7 nm. By comparison of the textural properties under dry and wet conditions, both high specific surface area and pore volume were obtained in presence of water. No contribution of micropores was observed in any sample. The textural characterizations are in agreement with previous studies, where textural properties are enhanced under wet condition respect to dry condition [23,24].

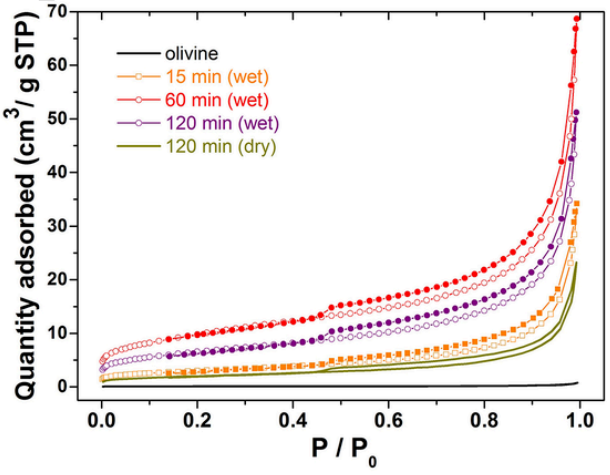

Fig. 3. N_2 adsorption/desorption isotherms of as-received olivine and as-milled olivine under wet and dry conditions in CO_2 atmosphere (PCO_2 = 1.0 atm).

Table 2
Textural parameters of the as-received olivine and after mechanochemical activation in CO_2atmosphere (PCO_2 = 1.0 atm).

Conditions (wet/ dry)	Milling time (min)	S_{BET} (m^2/g)	V_{meso} (cm^3/g) [b]	D_{av} (nm) [c]
Wet	0	~0.4	<0.001	–
Wet	15	10	0.051	3.6
Wet	60	33	0.105	3.9
Wet	120	22	0.078	3.7
Dry	120	7	0.034	3.5

[a] BET Specific surface area obtained from $0.10 < P/P_0 < 0.30$; [b] BJH Desorption cumulative volume of pores between 1.7 nm and 300 nm diameter; [c] BJH Desorption average pore diameter (4 V/A).

SEM observations of olivine powders before and after wet milling in CO_2 atmosphere evidence that strong changes in the morphology and size of the agglomerates occurred (Figs. 4A-D). The starting olivine is formed for dense agglomerates, with a wide size distribution from 80 to 350 μm (Fig. 4A). The agglomerates have irregular shapes, straight edges, with smooth and clean surfaces (Fig. 4B). In contrast, olivine powders after 120 min of wet milling in CO_2 show a strong decrease in the average agglomerate size as well as a modification in the agglomerate morphology. In fact, after wet milling olivine agglomerates are mostly fine, with average sizes lower than 50 μm and with some agglomerate of ~100 μm (Fig. 4C). The agglomerate edges are rounded and the surfaces are formed by rounded-shaped disaggregated particles (Fig. 4D). The agglomerate looks as a sponge.

Morphological comparison between olivine powders milled for 15 and 120 min shows minor differences (Fig. 5). Sharp angular particles up to 2-3 μm in size are still found as part of larger agglomerates after 15 min of wet milling; their presence is not evident after 120 min of wet milling. However, big agglomerates covered by disaggregated particles seem to remain even after 120 min of wet milling, evidencing that olivine powders are very resistant to milling (Fig. S3). Surface image of an olivine agglomerate after 15 min of milling shows the presence of particles of some microns. The elements present in olivine such as Si, O, Mg and Fe show a homogenous distribution. The oxygen element was used as a reference because it is present both in the olivine and $MgCO_3$ phases (see Fig. S4). Change in its color indicates a region with different topology. In addition, C is distributed uniformly on the surface and it shows that the carbonation reaction occurred.

3.3. Carbonation of olivine after wet milling in CO_2 atmosphere

To evaluate the carbonation process during mechanochemical processing of olivine, several runs for different milling times using 0.25, 0.5, 1.0 and 1.5 atm of CO_2 pressure were performed. The amount of CO_2 stored in each run was calculated using the total carbon content measured in the final product and determined by LECO analysis (Table S1). The calculations assume that the total carbon content detected by LECO in the sample is only associated with CO_2 sequestrated, subtracting the carbon content of the pristine olivine. The amount of CO_2

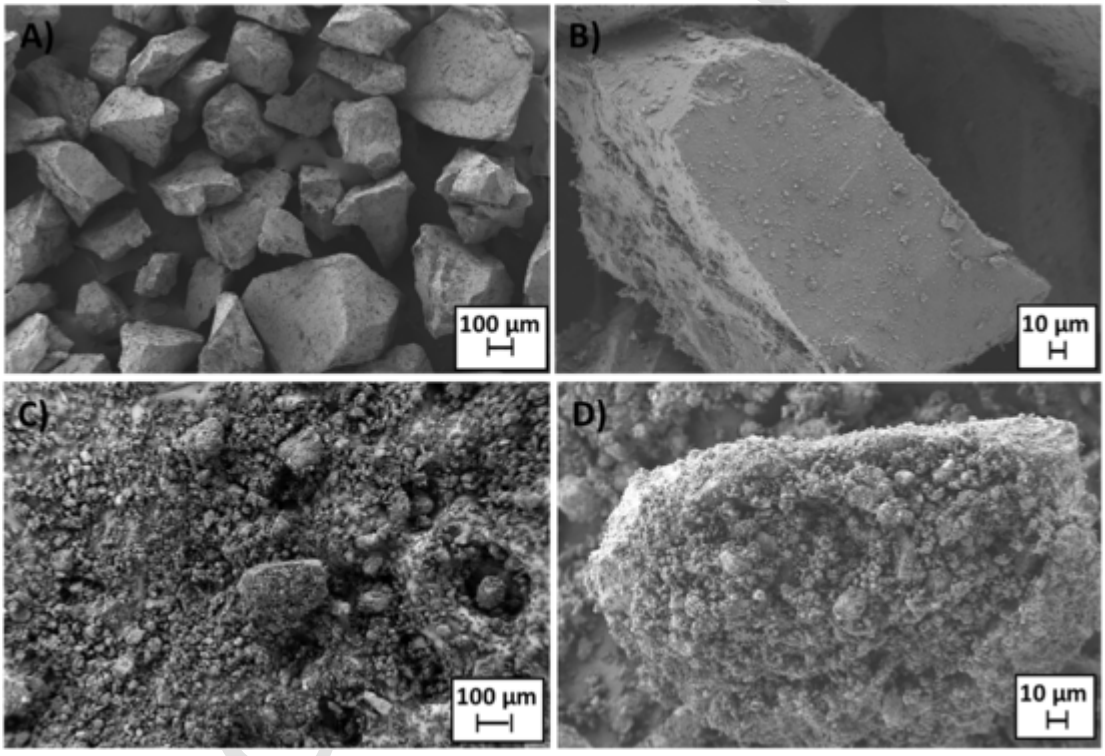

Fig. 4. SEM micrographs of the olivine powders: (A,B) as-received; (C,D) after 120 min of wet milling in CO_2 atmosphere (PCO_2 = 0.5 atm).

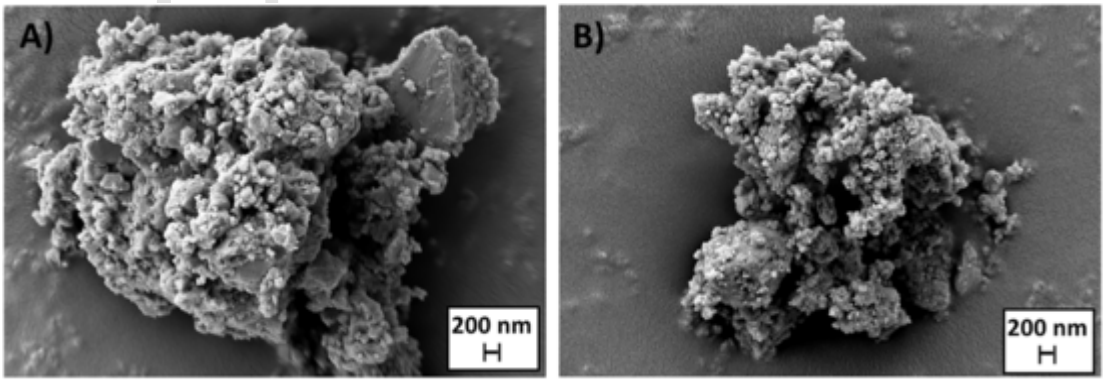

Fig. 5. SEM micrographs of the olivine powders after wet milling for: (A) 15 min, (B) 120 min in CO_2 (PCO_2 = 1.0 atm).

stored (wt%) and the mole ratio of CO_2 stored (in %) were estimated (Table S1). The maximum value of CO_2 (wt%) that can be stored at each CO_2 pressure was also shown (Fig. 6A). These data show the different influence of the milling time, CO_2 pressure and wet *versus* dry milling conditions on the carbonation of olivine. At short milling time (15 min), the CO_2 stored seems to be independent of CO_2 pressure, with values between 1.2 and 1.6 wt% for pressures between 0.25 and 1.5 atm of CO_2. However, when milling time progresses to 120 min, the wt% of CO_2 stored at a given CO_2 pressure also increases (Fig. 6A). As a general trend, the wt% of CO_2 stored grows with the CO_2 pressure between 0.25 and 1.0 atm, although it seems to be relatively constant for pressure between 1.0 and 1.5 atm. Wet milling for 120 min is enough to ensure a 50% of the mol ratio of CO_2 stored for all CO_2 pressures (Fig. 6B). This is an indication that the carbonation process of olivine in wet milling conditions was highly effective. By comparing of the mol ratio obtained using wet milling conditions (71%) with dry conditions (64%) at 1.0 atm of CO_2, the promotion effect of water was revealed on the CO_2 storage (Table S1). All these results demonstrate the successful dissolution of CO_2 in the olivine bulk assisted by mechanical activation in CO_2 atmosphere.

To analyze the evolution of the amount of CO_2 stored with the milling time and to correlate these values with the LECO analysis (Table S1), thermogravimetric measurements and MS analysis were performed (Fig. 7). Independently of the milling time, all curves display only weight loss due to the evolution of gaseous species. The weight loss increases with the milling time progress from 15 to 60 min (1.0 wt% to 6.3 wt%), and afterwards the weight loss remains constant (6.3–6.4 wt%). In particular, after 60 and 120 min of wet milling, three different weight loss processes in the temperature ranges of 50–160 °C, 160–450 °C and 450–900 °C, were identified. The coupled TGA-MS revealed that the evolved gases are water (H_2O) in the first temperature range, and carbon dioxide (CO_2) in all temperature ranges.

For the curve obtained after 60 min of milling, the first weight loss of about 2.8% was followed by losses of 3.2% and 0.3% for the second and third stages, respectively. Similar behavior was observed for the sample milled for 120 min, being the weight losses of each stage of 1.8, 3.4 and 1.2%, respectively. The first stage can be related mainly with dehydration, *i.e.* water desorption from the surface and bulk, as well as desorption of CO_2 physisorbed onto the olivine surface. The second stage is prominent and it is due to decarbonation of $MgCO_3$ to MgO [32]. The third stage involves CO_2 desorption from the partial dissolution of CO_3^{2-} ions/CO_2 molecules in a disordered silicate matrix with the increasing amorphization of the mineral [41]. Thus, there are three distinct kinds of CO_2 interaction with the olivine, concerning the three CO_2 peaks observed in the MS signal.

Moreover, if the weight loss of the first stage is mainly related to water evolution, 4.6% of CO_2 was released due to decarbonation process from olivine after 120 min of milling. This value is in good agreement with the wt% of CO_2 sequestrated calculated from the LECO analysis (Table S1). Regarding the first stage, there is a correlation between the weight loss value and the specific surface area of the sample (Table 2). In fact, the weight loss in the first stage is 2.8% and 1.8% for the samples milled 60 and 120 min, respectively, and their specific surface areas are 33 and 22 m^2/g. Similarly, other authors found that carbon dioxide adsorption with mechanically activated olivine increases with milling time and is proportional to the newly created surface [19,42]. The minor weight loss in the first stage for the sample milled 120 min evidences its dehydration after prolonged milling time, which explains their partial powder agglomeration.

Raman studies after wet milling of olivine for different times in 1.0 atm of CO_2 is shown in Fig. S5. All spectral signals obtained for olivine milled from 15 to 60 min can be assigned to Si—O vibrations of olivine structure and related with symmetric and anti-symmetric stretching vibrational modes of the SiO_4 ions [43,44]. Characteristic Raman peaks in olivine groups at ~820 and ~ 850 cm^{-1}, the "olivine doublet", show shifts as a function of cation substitution between forsterite and fayalite [43,44]. Bands at 822 and 855 cm^{-1} (Fig. S5) suggest that the olivine has a composition approximately 90% Forsterite and 10% Fayalite. This composition has a good match with the Rietveld refinement of the olivine XRPD pattern ($Fe_{0.2}Mg_{1.8}SiO_4$) [30].

The intensity of these bands progressively decreases as milling time increases, in correlation with olivine amorphization. Milling for 90 and 120 min induces the appearance of the G and D bands at 1605 and 1330 cm^{-1} due to graphite-like sp^2 and disordered sp^3 carbon bonds, respectively. The presence of carbonaceous species in the milled olivine for 120 min justify the minor difference between the weight loss due only to CO_2 released from carbonates in the TG measurement (since it is done under inert atmosphere) and the total carbon by LECO analysis (Fig. 7 and Table S1).

3.4. CO_2 hydrogenation of olivine after wet milling in CO_2 atmosphere

Mechanochemical activation of different Magnesium based materials in presence of water has been previously applied to induce CO_2 storage and/or CO_2 hydrogenation through complex reactions involv-

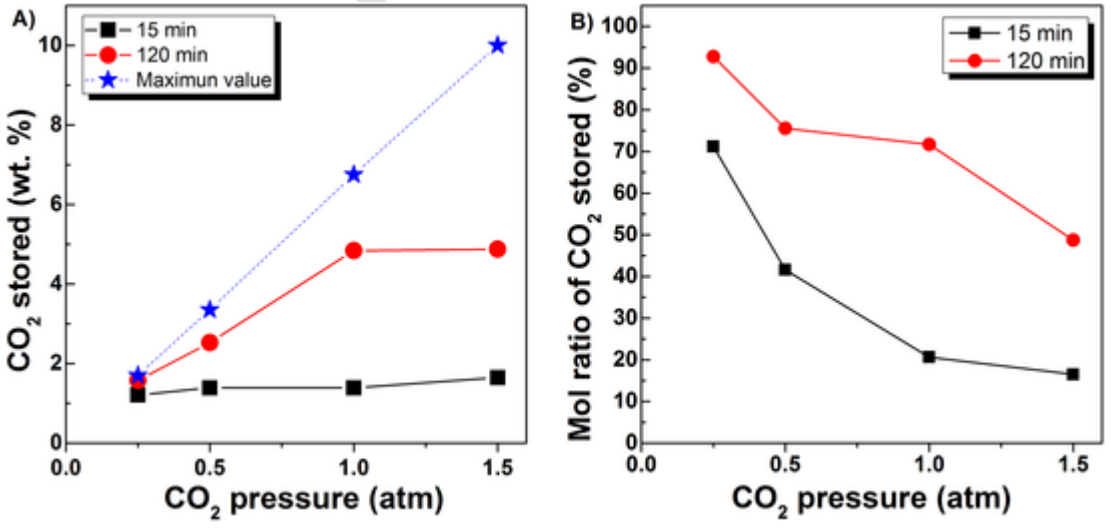

Fig. 6. (A) Amount of CO_2 stored (in wt%) and (B) mol ratio of CO_2 stored (in %) after wet milling of olivine as a function of CO_2 pressure.

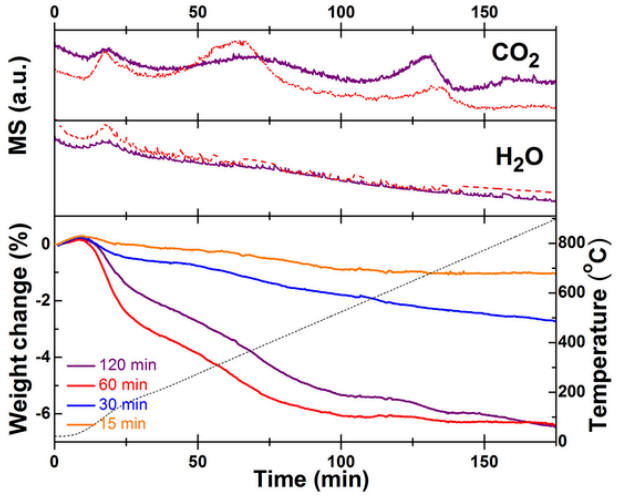

Fig. 7. Weight change (in %) and gas evolved (H_2O and CO_2) during heating of olivine after wet milling in CO_2 atmosphere (PCO_2 = 1.0 atm, heating ramp = 5 °C/min in Argon flow). MS signal: 60 min of milling (red color); 120 min of milling (violet color). (For interpretation of the references to color in this figure legend, the reader is referred to the web version of this article.)

ing solid-gas-liquid interfaces [32,33]. With this idea in mind, analysis of the gas evolved after wet milling of olivine in CO_2 atmosphere was carried out. Each spectrum was obtained after wet milling of a fresh olivine sample for a specified milling time and in a fix initial CO_2 pressure (Fig. 8A and B, Fig. S6). Independently of the starting CO_2 pressure, 15 min of milling are enough to promote CO_2 reduction ($\nu_{C=O}$ = 2350 cm^{-1}) as it can be inferred by the formation of CH_4 (ν_{C-H} = 3016 cm^{-1}, δ_{C-H} = 1305 cm^{-1}) and CO ($\nu_{C=O}$ = 2142 cm^{-1}). Complete consumption of CO_2 was observed after 30 min and 60 min of milling for 0.25 and 0.5 atm of CO_2 pressure, respectively (Fig. 8Aand Fig. S3). Under these conditions, prolonged milling for 1 h induces the formation of minor amounts of ethane and propane [45]. However, for higher CO_2 pressure it partially remains unreacted in the gas phase, in that case the milling progress does not induce the formation of C_xH_y species (Fig. 8B). No other IR-active gaseous compounds were detected above the impurity level in the experiments. It is important to mention that in the reference experiments (see §2.1) CO_2 is the only species detected in the gas phase, without evidence of CO_2 conversion.

Additionally, GC analysis were performed after 15, 60 and 120 min of olivine milling with 1.0 atm of CO_2 to consider the presence of non-active IR species. In addition to the previous identified CH_4, CO and CO_2 gaseous species, the presence of H_2 was also detected after 60 and 120 min of milling. Hydrogen was not detected before 15 min, probably due to an induction time necessary for its formation, as it was previously observed [32]. A yield of 90 mmoles H_2/kg olivine was obtained after 120 min of milling. Therefore, during wet milling it was observed the simultaneous formation of CH_4, CO and H_2 in the gas phase. The simultaneous formation of H_2 and CH_4 is in agreement with our recent works where olivine was milled using a spex mill [32,33].

The quantification of CH_4 and CO by FTIR as a function of milling time for different CO_2 pressure shows some general behaviors (Fig. 9). As milling time increases from 15 to 120 min, the yields of CH_4 and CO increase at different CO_2 pressure. In general, CO yield is lower than CH_4 yield at any milling time and CO_2 pressure. Moreover, the yield of CH_4 reaches a maximum value that seems to be independent of CO_2 pressure, but dependent of milling time. The maximum yields of CH_4 and CO are about 33 and 24 mmoles/kg olivine obtained after 120 min in 1.5 atm and 1.0 atm of CO_2, respectively. These gases were formed by a mechanism that promotes CO_2 reduction to CO (partial reduction) and CH_4 (complete reduction). Taking into account that during wet milling of olivine both CO_2 capture as well as CO_2 reduction processes are occurring, the results demonstrate that the multiple chemical reactions between olivine, water and CO_2 were promoted by mechanical energy input at room temperature.

3.5. CO_2 storage and conversion during wet milling: A comparison

Structural, microstructural and textural changes of olivine introduced with milling time progress result in a material readily dissolvable in acidic medium and activated for CO_2 storage [16]. The results reveal that adding water as milling aid promotes reactivity towards CO_2 sequestration (Table S1). Actually, after 15 min of wet milling, the amount of CO_2 stored was between 1.2 and 1.6 wt% for any CO_2 pressure, but only 0.1 wt% under dry conditions. At this time, the amount of CH_4 produced was very low (lower than 0.5% of CO_2 initial, see Fig. 9). Thus, the main reaction between olivine and CO_2 is the carbonation process (CCS), with a CO_2 storage rate of 0.33 mmoles•kg^{-1} olivine•sec^{-1} at 1 atm of CO_2.

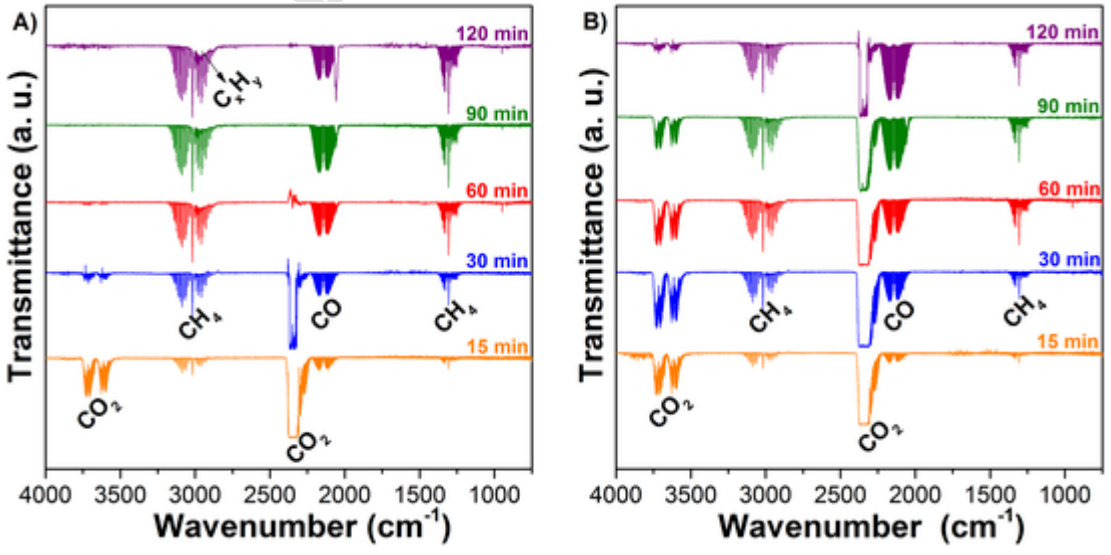

Fig. 8. Gas-phase FTIR spectra of the products formed after wet milling of olivine in CO_2 atmosphere for different milling times: (A) 0.5 atm, (B) 1.0 atm.

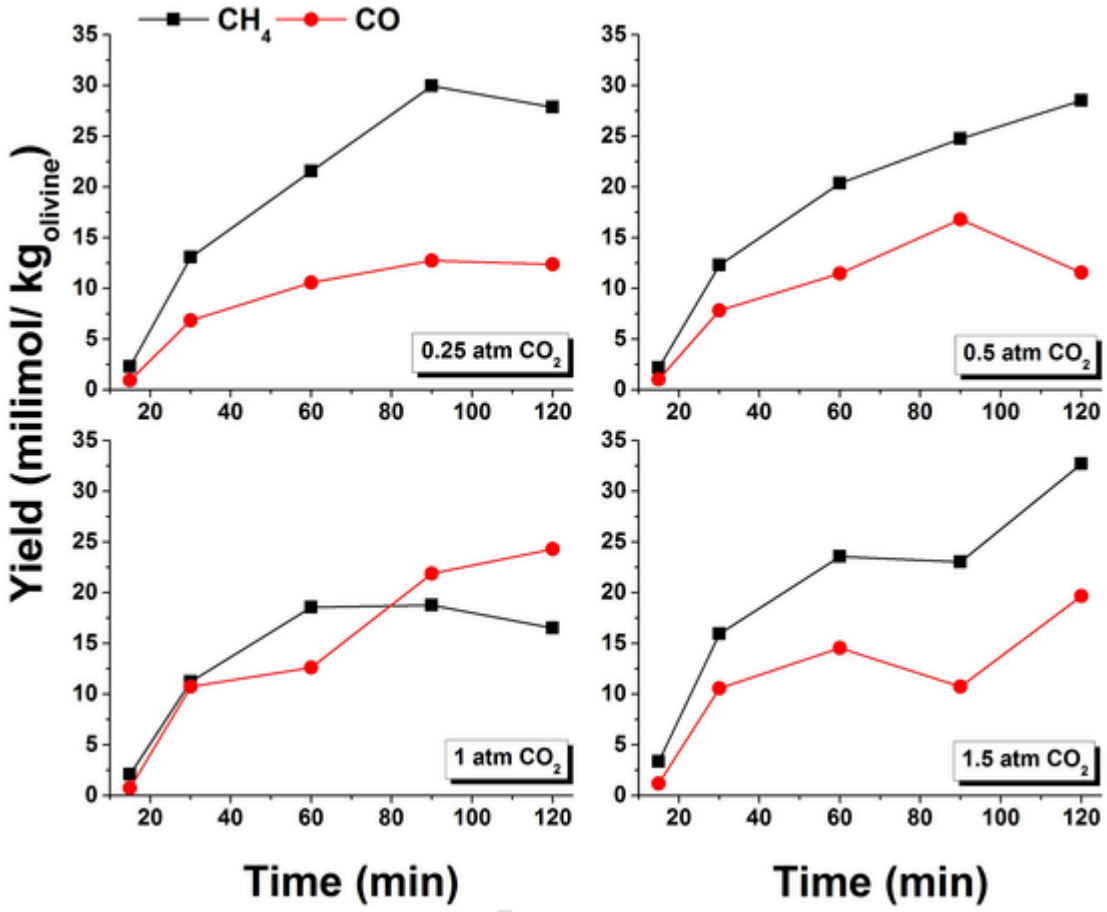

Fig. 9. CH_4 and CO yields during wet milling of olivine as a function of milling time for different CO_2 pressure. Yields of CH_4 and CO were quantified using mmol/kg olivine.

As milling time progresses, the amount of CO_2 sequestrated increases, being around 4.8 wt% after 120 min of milling at 1.0 atm of CO_2 (Figs. 6 and 7). Significant mol ratio of 90% and 70% of CO_2 stored for 0.25 and 1.0 atm of CO_2, respectively, were obtained in wet conditions (Fig. 6B). Considering that carbonation of olivine under dry condition gives a lower CO_2 mol ratio (64%, see Table S1) after 120 min of milling (reaction 1), we conclude that wet milling condition was effective to promote carbonation. It is important to highlight that the carbonation rate decreased from 0.33 to 0.15 mmoles CO_2•kg^{-1} olivine•sec^{-1} with the progress of milling time from 15 to 120 min at 1.0 atm of CO_2. This behavior can be related with the simultaneous occurrence of competitive reactions that retards the carbonation rate [46]. In fact, prolonged milling in CO_2 promotes not only the carbonation of olivine but also the hydrogen production and posterior reduction of CO_2 to CH_4 and CO (Fig. 9).

Direct comparison of CO_2 stored values of this study with others obtained by alternative carbonation processes is difficult because of the number of parameters that influence the carbonation performance. Table 3 summarizes the amount of CO_2 absorbed by different Mg-based silicates using milling, dissolution/carbonation processes and thermal chemisorption. Comparing the works where the olivine activation is done together with the mechanochemical carbonation, the wt% values achieved in this work after 120 min of wet milling olivine in CO_2 (1.0 and 1.5 atm) are superior to that previously reported using short milling time [20,42]. In addition, our values are also higher than those obtained after olivine activation (60 min) followed by dissolution/carbonation process for 120 min at 185 °C and 115 atm CO_2 [50]. In the olivine carbonation method that uses activation for long times (between 120 and 480 min) and posterior chemisorption of CO_2 at 500 °C, the amount of CO_2 stored was between 0.71 and 5.69 wt% depending on conditions used during wet milling [22,51]. Other processes involving mineral activation, high pressures (from 60 atm up to 260 atm) and temperatures (155–250 °C) report higher CO_2 storage capacity. Therefore, considering the mild conditions used in this work, *i.e.* room temperature, low CO_2 pressures (1.0 and 1.5 atm) and a total time of olivine treatment of 120 min and 180 min, the simultaneous olivine activation, dissolution and carbonation results in a promissory CO_2 sequestration process.

Regarding the CO_2 reduction mechanism to produce CH_4 and CO, two different cases can be considered depending on the initial CO_2 pressure. The first case involves the runs where CO_2 was completely consummated (Fig. 8A and S6). At this low CO_2 pressures (0.25 and 0.5 atm), milling for 90 and/or 120 min leads to the maximum amount obtained of CH_4 or CO. In these conditions, maximum CH_4 formation is only possible by transformation of some carbonaceous solid species present in the solid state in a H_2 environment. Previous investigations have shown that CH_4 can be formed during milling of carbonate phases [47] or inorganic carbon [48] in a H_2 rich atmosphere. The experimental evidence collected is not enough to clarify the main mechanism operating, but the reduction of $MgCO_3$ to CH_4 in a H_2 environment is highly possible. The second case corresponds to the experiments performed at 1.0 and 1.5 atm of CO_2. Wet milling of olivine in 1.0 atm of CO_2 leads to the formation of $MgCO_3$ and partial serpentinization (Figs. S2, 6 and 7), but as milling progress to 90 and 120 min, C was also detected in the solid phase (Fig. S5). The formation of C is possible through different reactions, such as Boudouard reaction among others [49]. In these conditions, simultaneous hydrogenation of carbon and/or methanation of CO_2 can be operating, promoted by Fe compounds to

Table 3
Mg-based silicates carbonation datasets summarizing experimental conditions of the mechanical activation, carbonation reaction, and amount of CO_2 stored (wt%).

Material	TA [a] (min)	Condition	CR [b]	TC [c] (min)	T (°C)	CO_2 [d] (atm)	$[CO_2]$ [e] (wt%)	Reference
Olivine	30	wet	M	30 (*)	RT	–	2.45	[42]
Olivine	60	dry	M	60 (*)	RT	5	3.96	[20]
Olivine	120	wet	M	120 (*)	RT	1	4.79	This study
Olivine	120	wet	M	120 (*)	RT	1.5	4.83	This study
Olivine	180	dry	M	180 (*)	RT	1	6.81	This study
Olivine	60	dry	HP	120	185	115	4.1	[50]
Olivine	60	Wet	HP	120	185	115	4.64	[50]
Fosterite	–	–	HP	60	185	150	29.7	[52]
Forsterite and lizadite	7.5	wet	HP	60	185	59	20	[53]
Forsterite and lizadite	120	dry	HP	60	185	59	13	[53]
Olivine	6	dry	HP	120–360	185	64	16–32	[54]
Olivine mine tailings	–	–	HP	36,000	200–250	129–260	11.44–32.05	[46]
Olivine	–	–	HP	4320	300	99	9.88	[55]
Forsterite and lizadite	7.5	wet	Ch	eq.	RT	1	0.27	[56]
Olivine basalt	120	10 wt% ethanol	Ch	30	500	gas flow (5%vol)	0.71	[22]
Olivine basalt	240	50 wt% ethanol	Ch	30	500	gas flow (5%vol)	0.97	[22]
Dunite (serpentine and Olivine)	480	wet	Ch	30	500	gas flow (5%vol)	5.7	[51]
Dunite (serpentine and Olivine)	120	10 wt% ethanol	Ch	30	500	gas flow (5%vol)	5.51	[51]
Dunite (serpentine and Olivine)	120	50 wt% ethanol	Ch	30	500	gas flow (5%vol)	5.69	[51]

MA: mechanically activated; Ch = chemisorption; M = milling; HT = high temperature treatment; HP = high-pressure reaction; eq = equilibrium;
[a] = time of material activation (TA); [b] = method used in carbonation reaction (CR); [c] = time of carbonation reaction (TC); [d] = initial conditions used in carbonation reaction; [e] = grams of captured CO_2 by 100 g of material. (*) the carbonation time is the same of mechanical activation because both are happening simultaneously.

produce CH_4 and CO. Thus, for high CO_2 pressures and long milling times, extension of carbonation reaction competes with hydrogen formation and posterior CO_2 reduction reactions.

As a general behavior, the maximum amount of CH_4 and CO was obtained between 90 and 120 min and its value seems to be relatively independent of the CO_2 pressure. Considering that both the milling energy input and the amount of water favor the splitting of water and the consequent H_2 formation, one of these factors probably limits the reaction progress. Both factors were kept constant in this study and a maximum of 33 mmoles/kg of CH_4 was obtained after 120 min under 1.5 atm of CO_2. By comparison with our previous work, same magnitude order of CH_4 (16 mmol/Kg) was obtained by milling 8 g of olivine/2 mL of water using a high energetic spex mill, but, differently, no carbon monoxide was detected [33]. However, when the amount of water was doubled at constant milling energy, the amount of CH_4 and others hydrocarbons significantly increases [33]. These results suggest the possibility to enhance the CCU process and avoid the partial reduction of CO_2 to CO. Future investigations using different amounts of water and energetic conditions during milling of olivine could help to promote the CH_4 formation without detrimental effect on CO_2 sequestration.

Finally, wet milling of olivine in CO_2 atmosphere showed to be an effective technique to promote mineral activation, dissolution and carbonation. Although it has been shown that the ball milling technique is energy consuming [16], main advantages are its wide applicability to other basaltic rocks abundant on the Earth's surface and the use of simple equipment under mild operation conditions: short milling time, room temperature and low CO_2 pressure. All these characteristics make wet grinding in CO_2 a technique with potential for large-scale carbon mineralization.

4. Conclusions

The processes of CO_2 storage in $MgCO_3$ and CO_2 conversion to CH_4 are investigated using olivine activated by wet mechanochemical milling under CO_2 atmosphere at room temperature. The milling times and CO_2 pressure were the factors evaluated in wet grinding. For comparison, specific dry milling experiments were also performed.

Under wet conditions, short milling times (15 min) promote mainly the CO_2 sequestration of 1.2–1.6 wt% and the formation of incipient amount of CH_4 and CO for any CO_2 pressure. In contrast, only 0.1 wt% of CO_2 was stored under dry milling, showing the role of water as milling aid in both sequestration and CO_2 reduction processes. As the milling time proceeds, carbonation reaction advances by obtaining the highest values (~4.8 and 6.8 wt%) for 1.0 atm of CO_2 after 120 min in wet milling and 180 min of dry milling, respectively. However, the carbonation rate decreases by a factor of 2 due to the fact that the CO2 conversion occurs simultaneously in wet milling, resulting in competitive processes. Maximum amounts of CH_4 and CO were produced after 120 min of milling, independently of the CO_2 pressure.

This study found evidence that after long wet mechanochemical processes in CO_2, microstructural, structural, and textural modification of the mineral occur. These changes promote the dissolution and partial serpentinization, and activation of olivine towards both CO_2 storage and reduction. Possible limiting factors of this reaction are the amount of water used and the energetic of the milling. Thus, further studies will be oriented to assist the olivine dissolution and reaction with CO_2 by modification of these parameters.

The results presented in this work give a scientific basis for further developing of CO_2 storage and utilization technologies using Mg-based silicates.

CRediT authorship contribution statement

Nadia Gamba: Data curation, Validation, Visualization, Formal analysis, Investigation, Writing - review & editing. **Valeria Farina:** Data curation, Validation, Visualization, Formal analysis, Investigation, Writing - review & editing. **Sebastiano Garroni:** Conceptualization, Methodology, Investigation, Writing - review & editing, Supervision, Funding acquisition. **Gabriele Mulas:** Conceptualization, Methodology, Investigation, Writing - review & editing, Supervision, Funding acquisition. **Fabiana Gennari:** Conceptualization, Methodology, Investigation, Writing - original draft, Writing - review & editing, Supervision, Funding acquisition.

Declaration of Competing Interest

None

Acknowledgements

The present work is part of the CO2MPRISE, "CO_2 absorbing Materials Project- RISE", a project that has received funding from the European Union's Horizon 2020 research and innovation programme, under the Marie Skłodowska-Curie Grant Agreement No 734873. The work was also supported by CONICET (Consejo Nacional de Investigaciones Científicas y Técnicas), ANPCyT– (Agencia Nacional de Promoción Científica y Tecnológica), CNEA (Comisión Nacional de Energía Atómica) and UNISS (Università degli Studi di Sassari). The authors also thank Bernardo Pentke (Departamento Fisicoquímica de Materiales, CAB- CNEA) for the SEM micrographs. S.G and G.M. also acknowledge UNISS for the financial support received within the program "fondo di Ateneo per la ricerca 2019. The activity of V.F. was supported by Sardinian Regional Government with the financial support of the PhD scholarship (P.O.R. Sardegna F.S.E. - Operational Programme of the Autonomous Region of Sardinia, European Social Fund 2014-2020 - Axis III Education and training, Thematic goal 10, Investment Priority 10ii), Specific goal 10.5.

Appendix A. Supplementary data

Supplementary data to this article can be found online at https://doi.org/10.1016/j.powtec.2020.09.039.

References

[1] Intergovernmental Panel on Climate Change, ed, Climate Change 2013 - The Physical Science Basis, Cambridge University Press, Cambridge, 2014, doi:10.1017/CBO9781107415324.
[2] R.S. Norhasyima, T.M.I. Mahlia, Advances in CO_2 utilization technology: a patent landscape review, J. CO2 Util. 26 (2018) 323–335, doi:10.1016/j.jcou.2018.05.022.
[3] J. Bujnicki, P. Dykstra, E. Fortunato, R.-D. Heuer, C. Keskitalo, P. Nurse, Novel carbon capture and utilisation technologies, 2018, doi:10.26356/CARBONCAPTURE.
[4] R.M. Cuéllar-Franca, A. Azapagic, Carbon capture, storage and utilisation technologies: a critical analysis and comparison of their life cycle environmental impacts, J. CO2 Util. 9 (2015) 82–102, doi:10.1016/j.jcou.2014.12.001.
[5] C. Fernández-Dacosta, V. Stojcheva, A. Ramirez, Closing carbon cycles: evaluating the performance of multi-product CO_2 utilisation and storage configurations in a refinery, J. CO2 Util. 23 (2018) 128–142, doi:10.1016/j.jcou.2017.11.008.
[6] D.Y.C. Leung, G. Caramanna, M.M. Maroto-Valer, An overview of current status of carbon dioxide capture and storage technologies, Renew. Sust. Energ. Rev. 39 (2014) 426–443, doi:10.1016/j.rser.2014.07.093.
[7] A. Sanna, M. Uibu, G. Caramanna, R. Kuusik, M.M. Maroto-Valer, A review of mineral carbonation technologies to sequester CO_2, Chem. Soc. Rev. 43 (2014) 8049–8080, doi:10.1039/c4cs00035h.
[8] J.M. Matter, P.B. Kelemen, Permanent storage of carbon dioxide in geological reservoirs by mineral carbonation, Nat. Geosci. 2 (2009) 837–841, doi:10.1038/ngeo683.
[9] S.J.T. Hangx, C.J. Spiers, Coastal spreading of olivine to control atmospheric CO_2 concentrations: a critical analysis of viability, Int. J. Greenh. Gas Control. 3 (2009) 757–767, doi:10.1016/j.ijggc.2009.07.001.
[10] M. Verduyn, H. Geerlings, G. van Mossel, S. Vijayakumari, Review of the various CO_2 mineralization product forms, Energy Procedia 4 (2011) 2885–2892, doi:10.1016/j.egypro.2011.02.195.
[11] R. Zevenhoven, M. Slotte, J. Åbacka, J. Highfield, A comparison of CO_2 mineral sequestration processes involving a dry or wet carbonation step, Energy. 117 (2016) 604–611, doi:10.1016/j.energy.2016.05.066.
[12] J.D. Rimstidt, S.L. Brantley, A.A. Olsen, Systematic review of forsterite dissolution rate data, Geochim. Cosmochim. Acta 99 (2012) 159–178, doi:10.1016/j.gca.2012.09.019.
[13] D. Wolff-Boenisch, S.R. Gislason, E.H. Oelkers, The effect of crystallinity on dissolution rates and CO_2 consumption capacity of silicates, Geochim. Cosmochim. Acta 70 (2006) 858–870, doi:10.1016/j.gca.2005.10.016.
[14] D. Tromans, J.A. Meech, Enhanced dissolution of minerals: stored energy, amorphism and mechanical activation, Miner. Eng. 14 (2001) 1359–1377, doi:10.1016/S0892-6875(01)00151-0.
[15] R.A. Kleiv, M. Thornhill, Mechanical activation of olivine, Miner. Eng. 19 (2006) 340–347, doi:10.1016/j.mineng.2005.08.008.
[16] J. Li, M. Hitch, Mechanical activation of magnesium silicates for mineral carbonation, a review, Miner. Eng. 128 (2018) 69–83, doi:10.1016/j.mineng.2018.08.034.
[17] P. Baláž, Extractive Metallurgy of Activated Minerals, Elsevier Science, 2000.
[18] E. Turianicová, P. Baláž, L. Tuček, A. Zorkovská, V. Zeleňák, Z. Németh, A. Šatka, J. Kováč, A comparison of the reactivity of activated and non-activated olivine with CO_2, Int. J. Miner. Process. 123 (2013) 73–77, doi:10.1016/j.minpro.2013.05.006.
[19] M. Fabian, M. Shopska, D. Paneva, G. Kadinov, N. Kostova, E. Turianicová, J. Briančin, I. Mitov, R.A. Kleiv, P. Baláž, The influence of attrition milling on carbon dioxide sequestration on magnesium-iron silicate, Miner. Eng. 23 (2010) 616–620, doi:10.1016/j.mineng.2010.02.006.
[20] K.L. Sandvik, R.A. Kleiv, T.A. Haug, Mechanically activated minerals as a sink for CO_2, Adv. Powder Technol. 22 (2011) 416–421, doi:10.1016/j.apt.2010.06.004.
[21] T.A. Haug, R.A. Kleiv, I.A. Munz, Investigating dissolution of mechanically activated olivine for carbonation purposes, Appl. Geochem. 25 (2010) 1547–1563, doi:10.1016/j.apgeochem.2010.08.005.
[22] I. Rigopoulos, K.C. Petallidou, M.A. Vasiliades, A. Delimitis, I. Ioannou, A.M. Efstathiou, T. Kyratsi, Carbon dioxide storage in olivine basalts: effect of ball milling process, Powder Technol. 273 (2015) 220–229, doi:10.1016/j.powtec.2014.12.046.
[23] R.A. Kleiv, M. Thornhill, The effect of mechanical activation in the production of olivine surface area, Miner. Eng. 89 (2016) 19–23, doi:10.1016/j.mineng.2016.01.003.
[24] A. Neubeck, N.T. Duc, D. Bastviken, P. Crill, N.G. Holm, Formation of H_2 and CH_4 by weathering of olivine at temperatures between 30 and 70°C, Geochem. Trans. 12 (2011) 6, doi:10.1186/1467-4866-12-6.
[25] T.M. McCollom, Laboratory simulations of abiotic hydrocarbon formation in Earth's deep subsurface, Rev. Mineral. Geochem. 75 (2013) 467–494, doi:10.2138/rmg.2013.75.15.
[26] H.P. Scott, R.J. Hemley, H.-K. Mao, D.R. Herschbach, L.E. Fried, W.M. Howard, S. Bastea, Generation of methane in the Earth's mantle: In situ high pressure-temperature measurements of carbonate reduction, Proc. Natl. Acad. Sci. 101 (2004) 14023–14026, doi:10.1073/pnas.0405930101.
[27] J.F. Kenney, V.A. Kutcherov, N.A. Bendeliani, V.A. Alekseev, The evolution of multicomponent systems at high pressures: VI. The thermodynamic stability of the hydrogen-carbon system: The genesis of hydrocarbons and the origin of petroleum, Proc. Natl. Acad. Sci. 99 (2002) 10976–10981, doi:10.1073/pnas.172376899.
[28] M.O. Schrenk, W.J. Brazelton, S.Q. Lang, Serpentinization, carbon, and deep life, Rev. Mineral. Geochem. 75 (2013) 575–606, doi:10.2138/rmg.2013.75.18.
[29] D.I. Foustoukos, W.E. Seyfried, Hydrocarbons in Hydrothermal Vent Fluids: The Role of Chromium-Bearing Catalysts, Science (80-.) 304 (2004) 1002–1005, doi:10.1126/science.1096033.
[30] C. Oze, Have olivine, will gas: Serpentinization and the abiogenic production of methane on Mars, Geophys. Res. Lett. 32 (2005) L10203, doi:10.1029/2005GL022691.
[31] C. Oze, L.C. Jones, J.I. Goldsmith, R.J. Rosenbauer, Differentiating biotic from abiotic methane genesis in hydrothermally active planetary surfaces, Proc. Natl. Acad. Sci. U. S. A. 109 (2012) 9750–9754, doi:10.1073/pnas.1205223109.
[32] V. Farina, N.S. Gamba, F. Gennari, S. Garroni, F. Torre, A. Taras, S. Enzo, G. Mulas, CO2 Hydrogenation Induced by Mechanochemical Activation of Olivine With Water Under CO2 Atmosphere, Front. Energy Res. 7 (2019), doi:10.3389/fenrg.2019.00107.
[33] F. Torre, V. Farina, A. Taras, C. Pistidda, A. Santoru, J. Bednarcik, G. Mulas, S. Enzo, S. Garroni, Room temperature hydrocarbon generation in olivine powders: effect of mechanical processing under CO2 atmosphere, Powder Technol. 364 (2019) 915–923, doi:10.1016/j.powtec.2019.10.080.
[34] D.W. Ohlberg, S.M. Strickler, Determination of Percent Crystallinity of Partly Devitrified Glass by X-Ray Diffraction, J. Am. Ceram. Soc. 45 (1962) 170–171, doi:10.1111/j.1151-2916.1962.tb11114.x.
[35] A.A. Stec, P. Fardell, P. Blomqvist, L. Bustamante-Valencia, L. Saragoza, E. Guillaume, Quantification of fire gases by FTIR: experimental characterisation of calibration systems, Fire Saf. J. 46 (2011) 225–233, doi:10.1016/j.firesaf.2011.02.004.
[36] S.M. Morrison, R.T. Downs, D.F. Blake, A. Prabhu, A. Eleish, D.T. Vaniman, D.W. Ming, E.B. Rampe, R.M. Hazen, C.N. Achilles, A.H. Treiman, A.S. Yen, R.V. Morris, T.F. Bristow, S.J. Chipera, P.C. Sarrazin, K.V. Fendrich, J.M. Morookian, J.D. Farmer, D.J. DesMarais, P.I. Craig, Relationships between unit-cell parameters and composition for rock-forming minerals on earth, Mars, and other extraterrestrial bodies, Am. Mineral. 103 (2018) 848–856, doi:10.2138/am-2018-6123.

[37] S.J. Louisnathan, J.V. Smith, Cell dimensions of olivine, Mineral. Mag. J. Mineral. Soc. 36 (1968) 1123–1134, doi:10.1180/minmag.1968.036.284.08.
[38] P. Baláž, E. Turianicová, M. Fabián, R.A. Kleiv, J. Briančin, A. Obut, Structural changes in olivine (Mg, Fe)2SiO4 mechanically activated in high-energy mills, Int. J. Miner. Process. 88 (2008) 1–6, doi:10.1016/j.minpro.2008.04.001.
[39] M.D. Dyar, T.D. Glotch, M.D. Lane, B. Wopenka, J.M. Tucker, S.J. Seaman, G.J. Marchand, R. Klima, T. Hiroi, J.L. Bishop, C. Pieters, J. Sunshine, Spectroscopy of Yamato 984028, Polar Sci. 4 (2011) 530–549, doi:10.1016/j.polar.2010.06.001.
[40] M. Thommes, K. Kaneko, A.V. Neimark, J.P. Olivier, F. Rodriguez-Reinoso, J. Rouquerol, K.S.W. Sing, Physisorption of gases, with special reference to the evaluation of surface area and pore size distribution (IUPAC technical report), Pure Appl. Chem. 87 (2015) 1051–1069, doi:10.1515/pac-2014-1117.
[41] E.V. Kalinkina, A.M. Kalinkin, W. Forsling, V.N. Makarov, Sorption of atmospheric carbon dioxide and structural changes of Ca and Mg silicate minerals during grinding, Int. J. Miner. Process. 61 (2001) 273–288, doi:10.1016/S0301-7516(00)00035-1.
[42] P. Turianicová, E. Baláz, A possible way to storage carbon dioxide on mechanically activated olivine (Mg, $Fe)_2SiO_4$, VI International Conference on Mechanochemistry and Mechanical Alloying (INCOME 2008), 2008 316–319 http://eprints.nmlindia.org/5147.
[43] K.E. Kuebler, B.L. Jolliff, A. Wang, L.A. Haskin, Extracting olivine (Fo-Fa) compositions from Raman spectral peak positions, Geochim. Cosmochim. Acta 70 (2006) 6201–6222, doi:10.1016/j.gca.2006.07.035.
[44] L.B. Breitenfeld, M.D. Dyar, C.J. Carey, T.J. Tague, P. Wang, T. Mullen, M. Parente, Predicting olivine composition using Raman spectroscopy through band shift and multivariate analyses, Am. Mineral. 103 (2018) 1827–1836, doi:10.2138/am-2018-6291.
[45] N. Makhoukhi, E. Péré, R. Creff, C. Pouchan, Determination of the composition of a mixture of gases by infrared analysis and chemometric methods, J. Mol. Struct. 744–747 (2005) 855–859, doi:10.1016/j.molstruc.2005.01.021.
[46] K. Kularatne, O. Sissmann, E. Kohler, M. Chardin, S. Noirez, I. Martinez, Simultaneous ex-situ CO2 mineral sequestration and hydrogen production from olivine-bearing mine tailings, Appl. Geochem. 95 (2018) 195–205, doi:10.1016/j.apgeochem.2018.05.020.
[47] B.-X. Dong, L. Wang, J. Zhao, Y.-L. Teng, C. Ping, W. Zhu, H.-B. Chen, W.-L. Liu, Highly selective room-temperature catalyst-free reduction of alkaline carbonates to methane by metal hydrides, Energy Technol. 7 (2019) 1800719, doi:10.1002/ente.201800719.
[48] M.L. Grasso, J. Puszkiel, L. Fernández Albanesi, M. Dornheim, C. Pistidda, F.C. Gennari, CO_2 reutilization for methane production via a catalytic process promoted by hydrides, Phys. Chem. Chem. Phys. 21 (2019) 19825–19834, doi:10.1039/C9CP03826D.
[49] J. Gao, Y. Wang, Y. Ping, D. Hu, G. Xu, F. Gu, F. Su, A thermodynamic analysis of methanation reactions of carbon oxides for the production of synthetic natural gas, RSC Adv. 2 (2012) 2358–2368, doi:10.1039/c2ra00632d.
[50] T.A. Haug, Dissolution and Carbonation of Mechanically Activated Olivine Thesis for the degree of Philosophiae Doctor 2010.
[51] I. Rigopoulos, M.A. Vasiliades, I. Ioannou, A.M. Efstathiou, A. Godelitsas, T. Kyratsi, Enhancing the rate of ex situ mineral carbonation in dunites via ball milling, Adv. Powder Technol. 27 (2016) 360–371, doi:10.1016/j.apt.2016.01.007.
[52] W.K. O'Connor, D.C. Dahlin, G.E. Rush, S.J. Gerdemann, L.R. Penner, D.N. Nilsen, Aqueous Mineral Carbonation: Mineral Availability, Pretreatment, Reaction Parametrics, and Process Studies, Doe/Arc-Tr-04-002, 2005 1–19, doi:10.13140/RG.2.2.23658.31684.
[53] J. Li, M. Hitch, Structural and chemical changes in mine waste mechanically-activated in various milling environments, Powder Technol. 308 (2017) 13–19, doi:10.1016/j.powtec.2016.12.003.
[54] J. Li, A.D. Jacobs, M. Hitch, Direct aqueous carbonation on olivine at a CO_2 partial pressure of 6.5 MPa, Energy 173 (2019) 902–910, doi:10.1016/j.energy.2019.02.125.
[55] J. Wang, N. Watanabe, A. Okamoto, K. Nakamura, T. Komai, Enhanced hydrogen production with carbon storage by olivine alteration in CO_2 -rich hydrothermal environments, J. CO2 Util. 30 (2019) 205–213, doi:10.1016/j.jcou.2019.02.008.
[56] J. Li, M. Hitch, Carbon dioxide adsorption isotherm study on mine waste for integrated CO_2 capture and sequestration processes, Powder Technol. 291 (2016) 408–413, doi:10.1016/j.powtec.2015.12.011.